

Effect of crystal surface orientation on aqueous solutions confined in charged nanopores by molecular dynamics simulations

Nghiên cứu ảnh hưởng của hướng bề mặt tinh thể đối với dung dịch nước ở trong ống nano tích điện bằng phương pháp mô phỏng động học phân tử

Nguyen Tu Khai Nam^{a,b}, Luc Han Tuong^c, Nguyen Thuy Uyen^d, Nguyen Phuoc The^b, Hoang Hai^{a,b*}
Nguyễn Tự Khải Nam^{a,b}, Lục Hán Tường^c, Nguyễn Thùy Uyên^d, Nguyễn Phước Thế^b, Hoàng Hải^{a,b*}

^aInstitute of Fundamental and Applied Sciences, Duy Tan University, 6 Tran Nhat Duat Street, District 1, Ho Chi Minh City 700000, Vietnam

^aViện Nghiên cứu Khoa học Cơ bản và Ứng dụng, Đại học Duy Tân, 6 Đường Trần Nhật Duật, Quận 1, Thành phố Hồ Chí Minh 700000, Việt Nam

^bFaculty of Environmental and Natural Sciences, Duy Tan University, 03 Quang Trung Street, Da Nang, Vietnam

^bKhoa Khoa học Môi trường và Tự nhiên, Đại học Duy Tân, 03 Đường Quang Trung, Đà Nẵng, Việt Nam

^cCao Thang Technical College, 65 Huynh Thuc Khang Street, District 1, Ho Chi Minh City, Vietnam

^cTrường Cao đẳng Kỹ thuật Cao Thắng, 65 Đường Huỳnh Thúc Kháng, Quận 1, Thành phố Hồ Chí Minh, Việt Nam

^dFaculty of Physics and Engineering Physics, Ho Chi Minh City University of Science, 227 Nguyen Van Cu Street, District 5, Ho Chi Minh City, Vietnam.

^dKhoa Vật lý và Vật lý Kỹ thuật, Đại học Khoa học Tự nhiên, 227 Đường Nguyễn Văn Cừ, Quận 5, Thành phố Hồ Chí Minh, Việt Nam

(Ngày nhận bài: 02/10/2023, ngày phản biện xong: 09/10/2023, ngày chấp nhận đăng: 16/10/2023)

Abstract

This study investigates the impact of crystal surface orientation on aqueous solutions confined in charged nanopores by using molecular dynamics simulations. Pore walls have been modeled as (100) and (110) silicon layers with the positively charged inner-most layer, while the aqueous solutions consist of only counter-ions and water. It has been shown that the crystal surface orientation has a noticeable influence on the properties of the aqueous solutions in the region close to the surface. The counter-ions and water molecules are more absorbed on the (110) surface than the (100) surface. The molecular diffusion coefficient of water molecules is greater in the vicinity of the (100) surface. In addition, the velocity of the aqueous solution induced by an external electric field is larger in the (100) nanopores. These behaviors are attributed to the greater surface density of the (110) surface. Furthermore, a comparison between simulation results with those computed from classical continuum theories has revealed that these theories provide quantitative predictions only in regions distant from the pore surfaces.

Keywords: Molecular dynamics simulations; electrical double layers; crystal surface orientations; nanopores; aqueous solutions.

Tóm tắt

Nghiên cứu này khám phá ảnh hưởng của hướng bề mặt tinh thể đối với dung dịch nước ở trong ống nano tích điện bằng phương pháp mô phỏng động học phân tử. Thành ống được mô hình hóa là các lớp silic (100) và (110) với lớp

*Corresponding Author: Hoang Hai

Email: hoanghai3@duytan.edu.vn

trong cùng mang điện tích dương, trong khi dung dịch nước chỉ gồm các ion đối kháng và nước. Nghiên cứu chỉ ra rằng hướng bề mặt tinh thể có một ảnh hưởng đáng kể đối với các tính chất của dung dịch nước trong vùng gần bề mặt tinh thể. Ion đối kháng và phân tử nước được hấp thụ nhiều hơn trên bề mặt (110) so với bề mặt tinh thể (100). Hệ số khuếch tán phân tử nước ở vùng sát bề mặt (100) là lớn hơn. Thêm nữa, vận tốc của dung dịch nước do điện trường bên ngoài gây ra lớn hơn trong ống nano (100). Những đặc tính này có thể được quy cho mật độ bề mặt của tinh thể silic theo hướng (110) lớn hơn. Hơn nữa, việc so sánh kết quả mô phỏng với các lý thuyết môi trường liên tục cơ bản đã chỉ ra rằng những lý thuyết này chỉ dự đoán các thuộc tính với độ chính xác đáng kể trong vùng xa bề mặt ống nano.

Từ khóa: Mô phỏng động học phân tử; Lớp kép điện; Hướng bề mặt tinh thể; Ống nano; Dung dịch nước.

1. Introduction

The investigation of thermophysical properties of aqueous solutions confined in micro- and nano-pores has gained much interest in diverse scientific disciplines from fundamental sciences to engineering applications such as drug delivery and lab-on-a-chip systems [1-3]. In such systems, since the surface-to-volume ratio is high and the characteristic dimensions are comparable to the molecular size, surface characteristics, such as the geometric surface, and the sign of surface charge, etc, have strong effects on the thermophysical properties of the confinement aqueous solution [1-2]. As a consequence, these properties exhibit significantly different from those in the bulk state, particularly in a region close to the surfaces [1-2, 4]. Classical continuum theories (CCT) are unable to adequately describe or predict these effects [5-8], while experimental approaches are incapable of providing molecular insights into these phenomena [1-2, 4].

With advancements in computer science, molecular simulation has emerged as a powerful tool for investigating properties of systems at the micro- and nano-scales [9-11]. This tool relies on a molecular representation of systems and can yield reliable results for well-defined ones. Many surface effects on aqueous solutions within nanopores have been elucidated thanks to molecular simulations [5-8, 12-15]. Boek et al. [12] performed molecular simulations to investigate the effect of surface orientation on the structural properties of water on the surface of crystalline ureas. Lee et al. [13] conducted a simulation investigation into

the structure and dynamic properties of liquid water on hydrophobic and hydrophilic surfaces. The effects of surface charge, including intensity, distribution, and sign [5-6, 14-15], have been also investigated through molecular simulations. These simulation studies have found that the structure and dynamic properties of aqueous solutions within the region adjacent to the surface are strongly influenced by surface characteristics.

While many studies have already reported on surface effects in the literature [1-2, 4, 5-8, 12-15], a plethora of surface characteristics remain unexplored due to their diversity [1-2, 4]. In addition, silicon has been widely used in lab-on-a-chip systems [1-3, 16]. Therefore, the primary objective of this work is to investigate the influence of charged silicon surface orientation at an ambient condition. Furthermore, it evaluates the capacity of CCT to predict the static and dynamic properties of aqueous solutions on these surfaces.

The rest of paper is structured as follow. Molecular simulation is detailed in Section II. Then, in section III the simulation results are presented and discussed. Finally, main findings are summarized in Section IV.

2. Molecular simulations

2.1. Molecular model

The solid walls are composed of silicon layers where the atoms are fixed in their original lattice positions. These two walls are separated by 26 \AA , forming a nanopore. The silicon atoms on the inner-most layers are positively, partially and uniformly charged with the magnitude of surface density of 0.181 C/m^2 .

To investigate the effect of crystal surface orientation, we have considered two kinds of orientation walls, i. e. (100) and (110) directions, as illustrated in Fig. 1. For simplicity, the aqueous solutions studied were assumed to be composed of negatively charged Chloride ions and water molecules [5-7, 15]. A schematic of the simulation box is provided in Fig. 1.

The water is modeled by using the SPC/E model [17], which comprises two sites for hydrogen atoms and one site for oxygen atom, as shown in Fig. 1. In this model, both of charge and mass are positioned at each site, constituting a three-site model. The O-H bond length and the H-O-H angle are held rigid at 0.1 nm and 109.47° , respectively. The charge of oxygen atom is of $-0.8476e$, while the hydrogen atom carries a charge of $+0.4328e$. For the Cl ions and Si atoms, the charged Lennard-

Jones (LJ) atom model has been employed to represent them [5-6]. Thus, the interaction potential between atoms is computed by:

$$u_{ij} = 4\varepsilon_{ij} \left[\left(\frac{\sigma_{ij}}{r_{ij}} \right)^{12} - \left(\frac{\sigma_{ij}}{r_{ij}} \right)^6 \right] + \epsilon \frac{q_i q_j}{r_{ij}} \quad (1)$$

where ε_{ij} and σ_{ij} are the LJ parameters respectively representing the potential well depth and the collision diameter, r_{ij} is the distance between the atoms, ϵ is the Coulomb's constant, q_i is the charge of atom. The LJ parameters of atoms ($\varepsilon_{ij}, \sigma_{ij}$) are detailed in Table 1.

For unlike fluid atoms, the standard Lorentz–Berthelot combining rules were employed to determine the LJ parameters as [18-19]:

$$\varepsilon_{ij} = \sqrt{\varepsilon_{ii} \varepsilon_{jj}} \quad (2a)$$

$$\sigma_{ij} = \frac{(\sigma_{ii} + \sigma_{jj})}{2} \quad (2b)$$

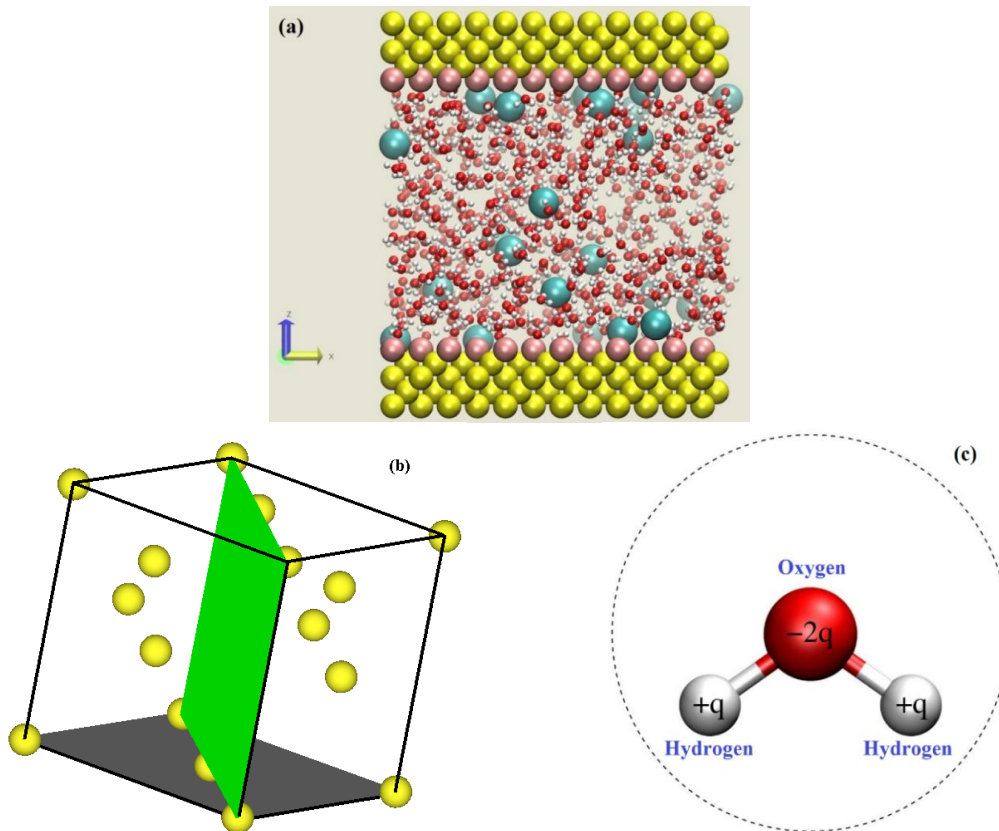


Figure 1: (a) Schematic representation of a nanopore containing water molecules and Cl counter-ions: Oxygen atoms (in red), Hydrogen atoms (in white), Cl counter-ions (in cyan), Charged Si atoms (in pink), and Non-charged Si atoms (in yellow). (b) A unit cell of the diamond cubic crystal structure for silicon and the orientations of the surface structures: (100) plane (highlighted in a dark color plane) and (110) plane (highlighted in a green color plane). (c) The SPC/E model for the water molecule.

Table 1: Lennard-Jones potential parameters of atomic species in the simulation system.

Species	ε (kJ/mol)	σ (\AA^0)
O	0.645	3.17
H	0.000	0.00
Cl	0.445	4.45
Si	2.44	3.37

2.2. Simulation details

Molecular dynamics (MD) simulations were conducted to determine the static and dynamic properties of the aqueous solution confined in the charged Si nanopore, which consists of four steps. First, the system was equilibrated during 0.5 ns. Then, the sampling was executed over a period of 1.5 ns to compute the static and diffusion properties. In the third step, an electric field strength was applied to the system along the x direction and the MD simulation continued for 1.5 ns to reach a steady state. Finally, a run of 2.0 ns was performed to calculate the velocity of aqueous solution.

To describe the motion of water molecules, we have decomposed it into two entirely independent components: translational motion and rotation about the center of mass [9]. Otherwise, the motion of ions was solely characterized by translation [9]. In addition, a combination of quaternion coordinates with Euler angles was employed to efficiently describe the rotational motion of water molecules [9]. The equations of motion were integrated by using the leap-frog Verlet algorithm with the time step of 1.0 fs [9-10]. To keep the temperature of the aqueous solution at an ambient condition of $T=300\text{K}$, the Berendsen thermostat was employed to adjust three velocity components for the MD simulations without the application of the external electric field, whereas it was applied to only two components perpendicular to the field

when it is present in the systems [20]. Classical periodic boundary conditions were applied in the x and y directions. The LJ potential interactions were calculated by truncation at a cutoff radius of 10.0 \AA^0 [9-10]. For the calculation of Coulomb potential interactions, the EW3DC (three-dimensional Ewald summation with the correction term) proposed by Yeh and Berkowitz was employed, in which the vacuum space added is of 72 \AA^0 [21]. In addition, an FFT grid spacing of 0.1nm and a TSC (triangular-shaped cloud, 2nd order) for the charge distribution and the force interpolation were chosen to compute the reciprocal-space interaction [22-23]. To compute density and velocity profile across the nanopore, the simulation box was uniformly divided into the x - y plane bins having the width of $\Delta z \approx 0.3 \text{ \AA}^0$.

The MD simulations were carried out by using an in-house FORTRAN code, which was validated and utilized to investigate the static and dynamic properties of various fluids confined in nanopores [7, 15, 24].

3. Results and discussions

3.1. Structure properties

Figure 2 shows the density profiles of water and Cl ion across the nanopore. Interestingly, results indicate that the crystal surface orientation has non-negligible effect on the density distribution of water and Cl ion in the vicinity of the surface. More precisely, the water and Cl ion are more strongly absorbed on the (110) surface than the (100) surface, as evidenced by the larger magnitude of the first peak. This behavior is probably attributed to the Si surface density. The (110) surface possesses a surface density of $0.0959 \text{ Atom/\AA}^2$, while it is of $0.0678 \text{ Atom/\AA}^2$ for the (100) surface [25].

In addition, the capability of a classical continuum theory to predict the counter-ion distribution has been evaluated. The theory considered in this study is a combination of the

Poisson equation and the Boltzmann distribution, which is detailed in Appendix. Figure 3 presents a comparison between the counter-ion concentration profiles obtained from the MD simulations and the CCT for the (100) surface. The results clearly indicate that the CCT can provide quantitative results only in regions distant from the surface, while it yields

a noticeable deviation in the region near the surface. This behavior is similar to results reported in the literature [5-8], which was already explained due to the limitations of this equation in accounting for factors such as the finite size of molecules and the polarization of water molecules, etc. [6, 8].

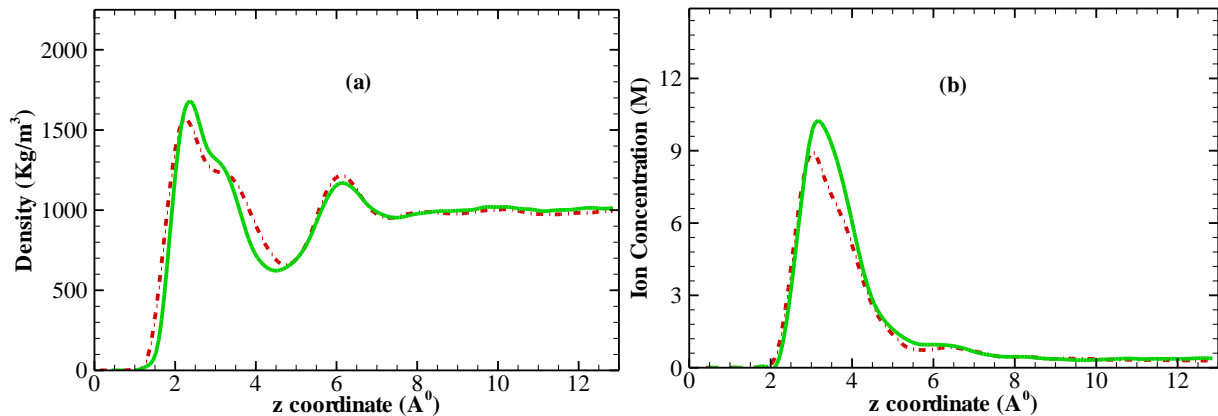


Figure 2: (a) Water density and (b) Counter-ion concentration profiles across the nanopores obtained from the MD simulations. (Red color) Dashed-Dotted lines correspond to the (100) nanopore. (Green color) Solid lines correspond to the (110) nanopore.

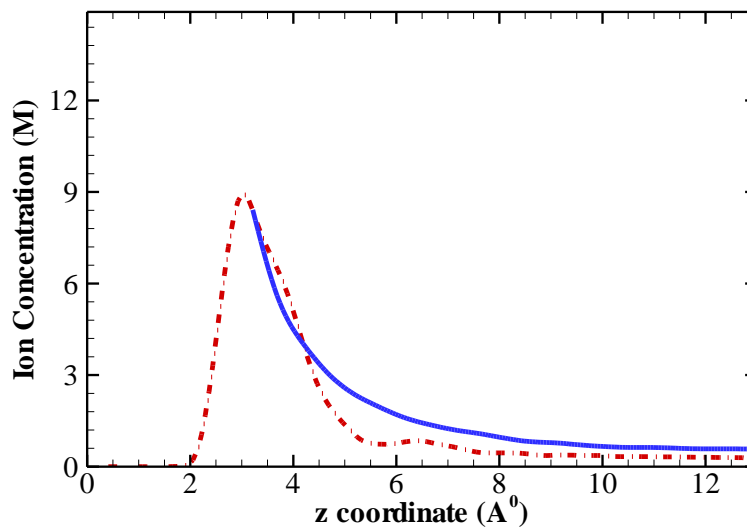


Figure 3: Counter-ion concentration profiles across the (100) nanopore obtained from the MD simulations (Dashed-Dotted line with Red color) and the CCT (Dashed-Dotted line with Blue color)

3.2. Dynamic properties

3.2.1. Diffusion coefficients

As presented in the previous section, the crystal surface orientation has non-negligible effects on the structural properties of the aqueous solution in the region close to the

surface. Therefore, this section focuses exclusively on the effect of crystal surface orientation on molecular diffusion in this region. The molecular diffusion coefficient was computed by using the Green-Kubo relation as [9-10]:

$$D = \frac{1}{d} \int_0^{\infty} c_v(t) dt \quad (3)$$

where, d is the dimensionality, t is the time, and c_v the velocity autocorrelation function (VACF) that is given as:

$$c_v(t) = \langle v(t)v(0) \rangle = \left(\frac{1}{N} \sum_{i=1}^N v_i(t)v_i(0) \right) \quad (4)$$

where v is the translational velocity, and N is the number of molecules. The molecular diffusion coefficients of the water molecules in the z direction and on the x - y plane for the two crystal surfaces computed from the MD simulations are given in Table 2.

Results clearly indicate that the molecular diffusion coefficient in the z direction is smaller than that on the x - y plane in both the crystal surface orientations. This behavior is consistent with the findings reported in the literature [7,

15, 26]. It was explained as the strong constraint imposed by the pore walls on the motion of water molecules in the z -direction [7, 15, 26].

Regarding the effect of crystal surface orientation, the simulation results clearly demonstrate its significant effect on the molecular diffusion coefficient of water molecules. To be more specific, the diffusion coefficient is smaller on the (110) surface compared to the (100) surface, particularly the molecular diffusion on the x - y plane. This difference can be attributed to the effect of water density [27]. As presented in the previous section, the water density on the (110) surface is higher than that on the (100) surface.

Table 2: Self-diffusion coefficient of water molecules in the region of the first peak.

	$D_{x-y} (10^{-9}m^2/s)$	$D_z (10^{-9}m^2/s)$
In the (100) nanopore	1.50±0.15	1.17±0.11
In the (110) nanopore	1.35±0.12	1.14±0.10

3.2.2. Velocity profile

The velocity profiles of aqueous solution confined in the pores induced by the external electric field, obtained from the MD simulations, are illustrated in Fig. 4. Results show that the velocity is greater in the (100) surface pore than in the (110) surface pore. This implies that the crystal surface orientation has an impact on the velocity. This behavior can be explained as follows. As presented above, the density is smaller in the (100) surface pore, resulting in reduced viscosity compared to the (110) surface pore.

Finally, the capability of a CCT to predict the velocity has been investigated. To do so, we

have considered a CCT that combines the Poisson equation, the Boltzmann distribution, and the Stokes equation. A comprehensive description of this CCT is available in the Appendix. A comparison between the velocity profiles computed from the MD simulation and the CCT for the (100) surface pore is presented in Fig. 5. Results show that the CCT exhibits noticeable deviations in the region proximate to the surface but yields reasonable results in regions distant from the surface. This observation underscores the limitations inherent to the CCT, as discussed previously [6-8], due to the effects of the finite size of molecules and polarisation of water molecules, etc.

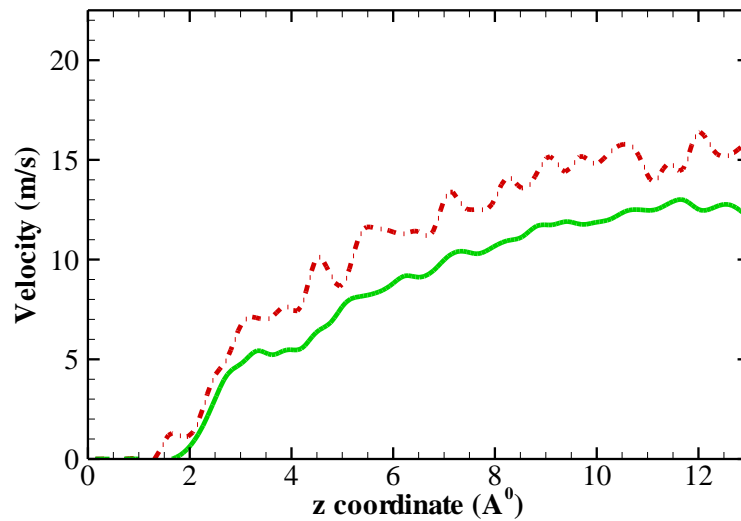


Figure 4: Velocity profiles across the nanopores obtained from the MD simulations. The legend is the same as that in Fig. 2.

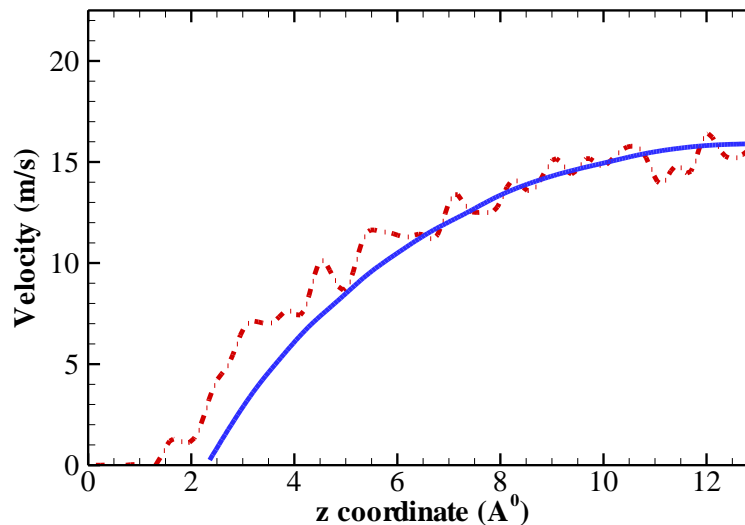


Figure 5: Velocity profiles across the (100) nanopore obtained from the MD simulations (Dashed-Dotted line with Red color) and the CCT (Dashed-Dotted line with Blue color)

4. Conclusions

In this study, we have investigated the influence of crystal surface orientation on the structural and dynamic properties of aqueous solutions confined within nanopores. In addition, the capability of classical continuum theories to predict these properties has been also evaluated. To achieve these, molecular dynamics simulations have been performed. For simplicity, the pore walls were modeled as the Silicon layers with the positively charged inner-most layers, in which the two types of crystal surface orientations, (100) and (110), have been considered. And, the aqueous

solutions are composed of only the Chloride counter-ions and water.

First, the density profiles of water and counter-ions were explored. The simulation results have indicated that both water and counter-ion are more absorbed on the (110) surface compared to the (100) surface, which can be attributed to the Si surface density. In addition, the CCT has been shown to yield quantitative results for the counter-ion distribution only in the region distant from the pore surface but exhibits significant deviations in the vicinity of the pore surface.

Then, we have exclusively focused on the effect on the molecular diffusion of water molecules in the proximity of the pore surface. It has been shown that the diffusion coefficient is higher on the (100) surface than on the (110) surface. This is probably the consequence of stronger density on the latter surface.

Finally, the velocity of the aqueous solutions induced by an external electric field was studied. The simulation results have shown that the velocity is greater in the (100) surface nanopore compared to the (110) surface nanopore, which is consistent with the observed density differences. In addition, the simulation velocity has been compared to that computed from the CCT. It has been found that the CCT yields reasonable results in the region far from the surface but exhibits noticeable deviations in the region close to the surface.

Appendix

In this appendix, classical continuum theories on electrical double layer (EDL) are presented. Under the assumption of the continuum model, the EDL can be described by solving the PB equation [28]. The PB equation is a combination of the Poisson equation and the Boltzmann distribution. A Boltzmann distribution for ion density and the PB equation for the electric-static potential are:

$$\nabla^2 \psi = -\frac{e \times n}{\tilde{\epsilon}} \quad (A1)$$

$$n = n_{\infty} \exp\left(-\frac{e \times \psi}{k_B T}\right) \quad (A2)$$

where, n is the number density of the counter-ion, n_{∞} is the number density of the counter-ions at the nanopore center, e is the electron charge, ψ is the electrostatic potential, k_B is the Boltzmann constant, T is the fluid temperature, and $\tilde{\epsilon}$ is the permittivity of the solvent. Substituting Eq. (A1) into Eq. (A2), one has:

$$\nabla^2 \psi = -\frac{e}{\tilde{\epsilon}} \times n_{\infty} \exp\left(-\frac{e \times \psi}{k_B T}\right) \quad (A3)$$

Integrating this equation with the boundary conditions of electric potential as $\frac{d\psi}{dz} = 0$ and $\psi=0$ at $z = z_c$, where z_c is the z coordinate of the pore center, it gives:

$$\frac{d\psi}{dz} = \sqrt{\frac{2k_B T n_{\infty}}{\epsilon}} \left[\sin\left(-\frac{e\psi}{k_B T}\right) - 1 \right]^{\frac{1}{2}} \quad (A4)$$

$$\psi = \frac{k_B T}{e} \ln \left[\cos^2 \left(\sqrt{\frac{n_{\infty} e^2}{2 \tilde{\epsilon} k_B T}} (z - z_c) \right) \right] \quad (A5)$$

Then, the number density of the counter-ion is written as:

$$n(z) = n_{\infty} \frac{1}{\cos^2 \left(\sqrt{\frac{n_{\infty} e^2}{2 \tilde{\epsilon} k_B T}} (z - z_c) \right)} \quad (A6)$$

In these equations, there is only one unknown value which is n_{∞} . To determine this quantity, the following boundary condition at the surface z_w can be used as [5-6, 26]:

$$\sigma_S = \tilde{\epsilon} \frac{d\psi}{dz} (z = z_w) \quad (A7)$$

Substituting Eqs. (A4) and (A5) into Eq. (A7), it can lead to an equation of n_{∞} as follows:

$$\sqrt{\frac{2k_B T n_{\infty}}{\epsilon}} \left[\frac{1}{\cos^2 \left(\sqrt{\frac{n_{\infty} e^2}{2 \tilde{\epsilon} k_B T}} (z_w - z_c) \right)} - 1 \right]^{\frac{1}{2}} = \frac{\sigma_S}{\tilde{\epsilon}} \quad (A8)$$

The quantity n_{∞} has been determined by numerically solving this equation thanks to the Newton-Raphson method [29].

The governing equation for the flow in nanopore under the electric field E_{Ext} without the pressure gradient is the one-dimensional Stokes equation as follows:

$$\frac{d}{dz} \left(\mu \frac{dv_F}{dz} \right) + enE_{\text{Ext}} = 0 \quad (A9)$$

Where μ is the viscosity of aqueous solution, and v_F is the velocity of aqueous solution. The boundary conditions for the flow are:

$$\frac{dv_F}{dz} (z = z_c) = 0 \text{ and } v_F(z = z_w) = 0 \quad (A10)$$

Substituting $n(z)$ in Eq. (A6) into Eq. (A9) and solving it, one has the analytical general solution as:

$$v_F = \frac{\epsilon^3 n_\infty^2 E_{Ext}}{2\mu \epsilon k_B T} \ln \left[\cos \left(\sqrt{\frac{n_\infty \epsilon^2}{2\epsilon k_B T}} (z - z_c) \right) \right] + C_1 \sqrt{\frac{n_\infty \epsilon^2}{2\epsilon k_B T}} (z - z_c) + C_2 \quad (A11)$$

where C_1 and C_2 are constants, which can be determined from the boundary conditions in Eq. (A10).

Acknowledgements

We are grateful to Prof. Yong Kweon Suh of Dong A university for his valuable discussions. We also thank Pau et Pays de l'Adour University and the MCIA for providing computational facilities.

References

- [1] Lyklema, J. (1995). *Fundamentals of interface and colloid science: Vol. 2 solid-liquid interfaces*. Academic Press.
- [2] Karniadakis, G., Beskok, A., & Aluru, A. (2005). *Microflows and nanoflows: fundamental and simulation*. Springer.
- [3] Abgrall, P., & Nguyen, N. T. (2008). "Nanofluidic devices and their applications". *Anal. Chem.*, 80(9), 2326-2341.
- [4] Israelachvili, J. (2010). *Intermolecular and surface forces* (3rd ed.). Academic Press.
- [5] Freund, B. (2002). "Electro-osmosis in a nanometer-scale channel studied by atomistic simulation". *J Chem. Phys.*, 116, 2194–2200.
- [6] Qiao, R., & Aluru, R. (2003). "Ion concentrations and velocity profiles in nanochannel electroosmotic flows. *J Chem Phys.*, 118, 4692–4701.
- [7] Hoang, H., Kang, S., & Suh, Y. K. (2010). "Molecular dynamics study on the effect of solution-wall interaction potential on the properties of solution in uniformly charged hydrophobic channel". *J. Mech. Sci. Technol.*, 24, 1401-1410.
- [8] Cazade, P. A., Hartkamp, R., & Coasne, B. (2014). "Structure and dynamics of an electrolyte confined in charged nanopores". *J Phys Chem C.*, 118, 5061–5072.
- [9] Allen, P., & Tildesley, J. (1987). *Computer Simulation of Liquids*. Clarendon Press, Oxford.
- [10] Frenkel, D., & Smit, B. (2001). *Understanding molecular simulation: from algorithms to applications* (2nd ed.). Academic Press.
- [11] Ungerer, P., Tavitian, B., & Boutin, A. (2005). *Applications of Molecular Simulation in the Oil and Gas Industry*. Technip.
- [12] Boek, E. S., Briels, W. J., van Eerden, J., & Feil, D. (1992). "Molecular-dynamics simulations of interfaces between water and crystalline". *J Chem. Phys.*, 96, 7010-7018.
- [13] Lee, H. S., & Rossky, J. (1994). "A comparison of structure and dynamics of liquid water at hydrophobic and hydrophilic surfaces - a molecular dynamics simulation study". *J. Chem. Phys.*, 100, 3334-3345.
- [14] Qiu, Y., & Chen, Y. (2014). "Counterions and water molecules in charged silicon nanochannels: the influence of surface charge discreteness". *Mol. Sim.*, 41, 1187.
- [15] Tran, T. H., Phan, G. T., Luc, H. T., Nguyen, P. T., & Hoang, H. (2020). "Molecular dynamics simulations on aqueous solution confined in charged nanochannels: asymmetric effect of surface charge". *Mol. Sim.*, 46(10), 796-804.
- [16] Craighead, H. (2006). "Future lab-on-a-chip technologies for interrogating individual molecules". *Nature*, 442, 387-393.
- [17] Berendsen, H. J. C., Grigera, J. R., & Straatsma, T. P. (1987). "The missing term in effective pair potentials". *J. Phys. Chem.*, 91, 6269.
- [18] Lorentz, H. A. (1881). "Ueber die Anwendung des Satzes vom Virial in der kinetischen Theorie der Gase". *Annalen der Physik*, 248, 127-136.
- [19] Berthelot, D. (1898). "Sur le mélange des gaz". *Comptes Rendus*, 126, 1703-1855.
- [20] Berendsen, H. J. C., Postma, J. P. M., van Gunsteren, W. F., Dinola, A., & Haak, J. R. (1984). "Molecular dynamics with coupling to an external bath". *J. Chem. Phys.*, 81, 3684.
- [21] Yeh, C., & Berkowitz, L. (1999). "Ewald summation for systems with slab geometry". *J. Chem. Phys.*, 111, 3155.
- [22] Toukmaji, A. Y., & Board Jr., J. A. (1996). "Ewald summation techniques in perspective: a survey. *Comput.* Phys. Commun., 95, 73.
- [23] Deserno, M., & Holm, C. (1998). "How to mesh up Ewald sums. II. An accurate error estimate for the particle-particle-particle-mesh algorithm". *J. Chem. Phys.*, 109, 7694-7701.
- [24] Hoang, H., Kang, S., & Suh, Y. K. (2009). "Molecular-dynamic simulation on the statical and dynamical properties of fluids in a nano-channel". *J. Comput. Fluids Eng.*, 13, 24.
- [25] Hull, R. (Ed.). (1999). *Properties of crystalline silicon* (No. 20). IET.

- [26] Kim, D., & Darve, E. (2006). "Molecular dynamics simulation of electro-osmotic flows in rough wall nanochannels". *Phys. Rev. E*, 73, 051203.
- [27] Poling, B. E., Prausnitz, J. M., & O'Connell, J. P. (2001). *The Properties of Gases and Liquids* (5th ed.). McGraw-Hill.
- [28] Petsev, D. N., van Swol, F., & Frink, L. J. (2021). *Molecular Theory of Electric Double Layers*. IOP Publishing.
- [29] Press, W. H., Teukolsky, S. A., Vetterling, W. T., & Flannery, B. P. (1992). *Numerical Recipes in Fortran* (2nd ed.). Cambridge University Press.